Supplementary material for: "Fluxes through steady chimneys in a mushy layer during binary alloy solidification"

DAVID W. REES JONES† AND M. GRAE WORSTER

Institute of Theoretical Geophysics, Department of Applied Mathematics and Theoretical Physics, University of Cambridge, Wilberforce Road, Cambridge, CB3 0WA, UK

(Received 23 July 2012)

The similarity solution for the active region near the chimney gives rise to a boundary-value problem. In this supplementary material, we restate the boundary-value problem in the planar geometry (section S1.1) and discuss the existence and uniqueness of solutions (section S1.2). This boundary-value problem is specified on the domain $[0, \delta]$, where the width of the active region δ is a free boundary that we determine dynamically in the full Chimney-Active-Passive-Zone model, in one of two ways. Firstly, we impose the chimney spacing, which indirectly imposes the width of the active region. We determine various asymptotic approximations for this case (section S2) and reach the important conclusion that the active region must have a finite width in order to sustain convection. Secondly, we impose the maximum-flux criterion to determine the width of the active region. We consider this case in the limit $\Omega \gg 1$, prove the existence and uniqueness of a chimney spacing that maximises the solute flux, and find its asymptotic dependence on Ω (section S3).

S1. The boundary-value problem in planar geometry

S1.1. *Statement of problem*

The similarity solution for the active region is governed by a fourth-order system of ordinary differential equations, subject to four boundary conditions, on the domain $[0, \delta]$. The governing equations are

$$\Theta'' = -\Psi\Theta' + \Psi'\Theta, \qquad \Psi'' = -\Theta', \tag{S1.1a, b}$$

and the boundary conditions are

$$\Psi_0'\Theta_0 = \Psi_0\Theta_0', \qquad \Theta_0' = \Psi_0\Theta_0/\Omega, \qquad \Theta_\delta = 1, \qquad \Theta_\delta' = 0. \tag{S1.2a, b, c, d}$$

The width of the active region must be determined both in the case of fixed chimney half-spacing L, and in the case in which L takes the value that maximises the solute flux (the *maximum-flux criterion* introduced in section 5).

In the case of imposing the chimney spacing, the size of the active region δ is determined through equation (3.13) in the main paper:

$$G(\delta, \Omega) = LR_m\theta_\infty^{1/2}, \tag{S1.3}$$

where

$$G(\delta, \Omega) = \Omega^{-1/2}(-\Psi_\delta')^{-1/2}\left(\delta - \Psi_\delta/\Psi_\delta'\right), \tag{S1.4}$$

which we can evaluate having solved the boundary-value problem (S1.1, S1.2).

† Email address for correspondence: dwr29@cam.ac.uk

In the case of imposing the maximum-flux criterion, we look for turning points which correspond to flux-maximising chimney spacings,

$$\frac{\partial \gamma}{\partial \delta} = 0, \tag{S1.5}$$

where γ is proportional to the solute flux through the chimney and satisfies

$$\gamma(\delta, \Omega) = \frac{1}{2}\frac{\Psi_0}{\Theta_0}\left(\delta - \Psi_\delta/\Psi'_\delta\right)^{-1}. \tag{S1.6}$$

In both cases, the solute flux is then determined by equation (3.16):

$$\mathcal{F}_{\text{Solute}} = -R_m \gamma(\delta, \Omega). \tag{S1.7}$$

S1.2. *Existence and uniqueness of solutions*

We first investigate the existence and uniqueness of solutions to the boundary-value problem as follows.

Given Ψ_0 and Θ_0, we can combine (S1.2a, b) to find Ψ'_0 and Θ'_0. This gives us an initial-value problem that we can solve on any domain $[0, \delta]$ (assuming the solution doesn't a singularity at a finite value of η). In this section, we restrict attention to $\Psi_0 > 0$ (which corresponds to flow into a chimney) and Θ_0 in the range $[0, 1]$ (since if $\Theta_0 > 1$, the depth of the mushy-layer near the chimney would be less than that in the passive region, contrary to experimental and numerical observations). However, this problem is well-posed for a wider class of initial conditions.

A solution of the boundary-value problem must satisfy boundary conditions (S1.2c, d). Therefore, we solve the initial-value problem introduced above to a high accuracy using the MATLAB 'ode113' routine, with relative and absolute error tolerances of 1×10^{-12} and 1×10^{-15} respectively. Then we use the MATLAB 'isosurfaces' routine to plot surfaces $\Theta_\delta = 1$, $\Theta'_\delta = 0$ (the required boundary conditions) as functions of Ψ_0, Θ_0 and δ. An example of this is shown in figure S1, and the solutions are the intersection curves highlighted. An alternative representation of these solutions can be obtained by taking slices through figure S1 at fixed values of δ. This corresponds to making contour plots, as shown in figure S2, and the solutions are the intersections of the contours $\Theta_\delta = 1$ and $\Theta'_\delta = 0$.

The solution branches can be categorised by the number of turning points of Ψ. The first branch (starting from the right of figure S1, that is going from low to high δ) has one turning point and each subsequent branch has an additional turning point. This corresponds to the fact that $\Psi' = 0 \Leftrightarrow \Theta'' = 0$ (from equation S1.1a). Physically, the number of turning points corresponds to the number of convecting cells within the active region. We have continued to higher values of δ and this pattern continues.

The first branch has a negative value of Ψ'_δ and thereafter the sign of Ψ'_δ alternates. Thus the 'even' branches correspond to flow from the active to the passive region, and therefore correspond to flow that is from the mushy layer into the liquid melt in the passive region. This is inconsistent with the boundary conditions at the mush–liquid interface (equation 3.2) and so is not a valid solution of the entire Chimney-Active-Passive-Zone model. Hence $G(\delta, \Omega)$ is defined only for $\Psi'_\delta < 0$. The other 'odd' branches (the third, fifth, and so on) are in principle permissible. However, they are not consistent with the overall Chimney-Active-Passive-Zone model in that the downwelling in the passive region was assumed to set the vertical velocity scale away from the chimney. Furthermore, these higher branches correspond to substantially lower-flux solutions of the full problem (as proved in the case $\Omega \gg 1$ in section S3). Therefore, motivated by

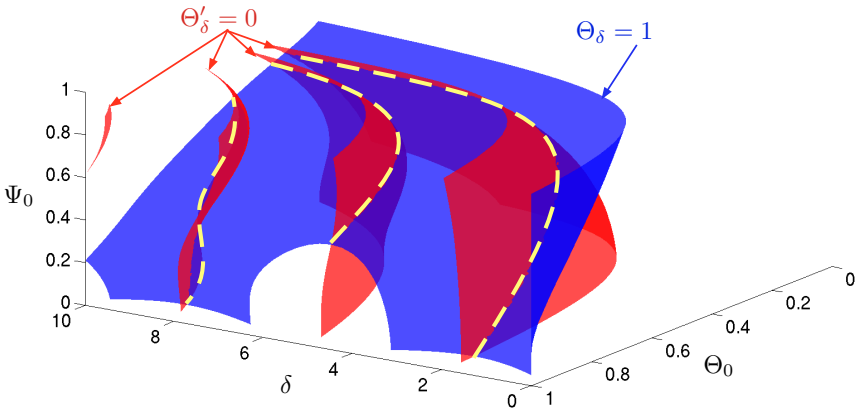

FIGURE S1. Surfaces $\Theta_\delta = 1$, $\Theta'_\delta = 0$ calculated in the case $\Omega = 1$. The intersection curves, highlighted with dashed yellow lines, correspond to branches of solutions.

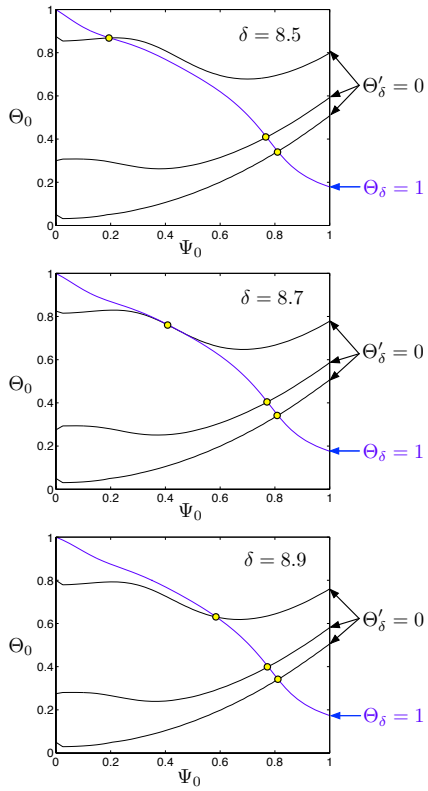

FIGURE S2. Contour plots at three values of δ at fixed $\Omega = 1$. At these values of δ, there are three intersection points, highlighted with yellow circles, corresponding the three branches in figure S1. Note that the third branch changes rapidly as a function of δ near $\delta = 8.7$ which corresponds to the contours lying approximately tangentially.

the maximum-flux criterion in section 5 of the main paper, we restrict attention to the first branch.

The first branch of solutions starts at $\Psi_0 = 0$, $\Theta_0 = 1$, $\delta = \pi/2$, and there are no solutions below $\delta = \pi/2$. This interesting cut-off occurs because the solutions are damped, nonlinear waves of frequency ω that is equal to a typical value of $\Theta^{1/2}$. But $\Theta < 1$, so $\omega < 1$. The first branch corresponds to $\omega\delta = \pi/2$ (one quarter wavelength), so $\delta > \pi/2$. This argument will be formalised in an asymptotic approximation below (section S2.2).

S2. The behaviour of the function $G(\delta, \Omega)$ in planar geometry – asymptotic analysis

S2.1. *Introduction*

In this section, we investigate the function $G(\delta, \Omega)$, which is proportional to the chimney spacing, in order to gain insight into the relationship between solute flux and chimney spacing. We consider two asymptotic limits for the width of the active region δ. We consider firstly the case δ is just above the lower cut-off at $\pi/2$, and secondly the behaviour at high values of δ. These limits can be considered in the context of fixed chimney spacing, which corresponds to imposing the value of $G(\delta, \Omega)$. Note that the asymptotic limits considered in this section do not correspond to the maximum solute flux.

S2.2. *Solution for $\delta = \pi/2 + \epsilon$ where $\epsilon \ll 1$*

There is an exact trivial solution of the boundary-value problem (S1.1, S1.2) for all values of δ (namely $\Theta \equiv 1$, $\Psi \equiv 0$), although G is not well-defined for this trivial solution, which corresponds to a stagnant mushy layer.

For $\delta > \pi/2$ there is a non-trivial solution. We compute its behaviour at $\delta = \pi/2 + \epsilon$ where $\epsilon \ll 1$ asymptotically by finding an asymptotic expansion of the solution in powers of ϵ. Let

$$\Theta = 1 + \epsilon g_1 + \epsilon^2 g_2 + O(\epsilon^3), \tag{S2.1}$$

$$\Psi = 0 + \epsilon f_1 + \epsilon^2 f_2 + O(\epsilon^3). \tag{S2.2}$$

We substitute these equations into the governing equations and boundary conditions and collect terms in powers of ϵ.

At $O(\epsilon)$, from (S1.1) the differential equations are

$$g_1'' = f_1', \qquad f_1'' = -g_1', \tag{S2.3a, b}$$

and from (S1.2) the boundary conditions are

$$f_1' = 0, \quad \Omega g_1' = f_1 \quad (\eta = 0), \qquad g_1 = 0, \quad g_1' = 0 \quad (\eta = \pi/2), \tag{S2.4a, b, c, d}$$

where we have used, for instance,

$$\begin{aligned} 1 = \Theta(\delta) = \Theta(\pi/2 + \epsilon) &= \Theta(\pi/2) + \epsilon\Theta'(\pi/2) + \frac{\epsilon^2}{2}\Theta''(\pi/2) + O(\epsilon^3) \\ &= \left[1 + \epsilon g_1 + \epsilon^2 g_2 + \epsilon(\epsilon g_1') + O(\epsilon^3)\right]_{\eta=\pi/2} \end{aligned}$$

At $O(\epsilon^2)$, from (S1.1) the differential equations are

$$g_2'' = -f_1 g_1' + f_1' g_1 + f_2', \qquad f_2'' = -g_2', \tag{S2.5a, b}$$

and from (S1.2) the boundary conditions are

$$f_2' + f_1' g_1 - f_1 g_1' = 0, \quad \Omega g_2' = f_1 g_1 + f_2 \quad (\eta = 0),$$

$$g_2 + g_1' = 0, \quad g_2' + g_1'' = 0 \quad (\eta = \pi/2). \tag{S2.6a, b, c, d}$$

S2.2.1. *Solution of the first-order problem*

The first-order equations are those of an unforced harmonic oscillator of frequency 1, which, to leading order, is the average value of $\Theta^{1/2}$, as discussed in the argument for the cut-off at $\delta = \pi/2$. We combine (S2.3a, b) and solve subject to boundary conditions (S2.4) – one of which is redundant because of the nature of the coupling – to find

$$f_1 = A(\Omega - 1 + \cos\eta), \tag{S2.7}$$

$$g_1 = -A(1 - \sin\eta), \tag{S2.8}$$

where A is an unknown constant that must be determined by solving the second-order problem.

S2.2.2. *Solution of the second-order problem*

The second-order problem has the character of an oscillator of frequency 1 that is resonantly forced by the first-order solution. This is evident upon eliminating g_2 between (S2.5a, b) and substituting equations (S2.7, S2.8) to obtain

$$f_2''' + f_2' = A^2[1 + (\Omega - 1)\cos\eta - \sin\eta]. \tag{S2.9}$$

We solve (S2.5a, b) subject to (S2.4a, b, c) to obtain

$$f_2 = -B\cos\eta + \frac{A^2}{2}\left[(\Omega - 1)(3\sin\eta - \eta\cos\eta) + \cos\eta + \eta\sin\eta + 2\eta\right] + C, \tag{S2.10}$$

$$g_2 = -f_2' + D, \tag{S2.11}$$

where

$$C = (\Omega - 1)(-B + A^2/2),$$
$$D = B + A^2\left[\pi(\Omega - 1)/4 + 1\right],$$

and B is another constant that could, in principle, be determined by proceeding to the next order. Finally, we apply (S2.4d) to find that

$$A^2\left[\frac{1}{2}(\Omega - 1) + \frac{\pi}{4}\right] - A = 0,$$

so $A = 0$, in which case the leading order solution is trivial, or

$$A = \left[\frac{1}{2}(\Omega - 1) + \frac{\pi}{4}\right]^{-1}. \tag{S2.12}$$

This means that we have fully determined the leading order problem and so can find the leading order behaviour of $G(\delta, \Omega)$.

S2.2.3. *Conclusions*

We can use this solution to compute the asymptotic behaviour of $G(\delta, \Omega)$, which gives

$$\begin{aligned} G(\delta, \Omega) &= 2\Omega^{-1/2}A^{-3/2}\epsilon^{-1/2} + O(\epsilon^{1/2}), \\ &= 2\Omega^{-1/2}\left[\frac{1}{2}(\Omega - 1) + \frac{\pi}{4}\right]^{3/2}\epsilon^{-1/2} + O(\epsilon^{1/2}). \end{aligned} \tag{S2.13}$$

In the special case $\Omega = 1$, this simplifies to

$$G(\delta, 1) = \frac{\pi^{3/2}}{4}\epsilon^{-1/2} + O(\epsilon^{1/2}). \tag{S2.14}$$

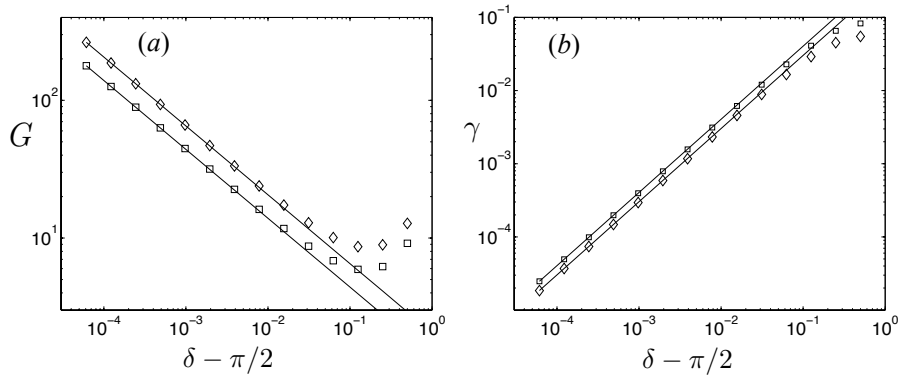

FIGURE S3. (a) is a log–log plot showing $G(\delta, \Omega)$ at $\Omega = 1$ (squares) and $\Omega = 2$ (diamonds). The asymptotic predictions from equation (S2.13) match extremely well (solid lines). Likewise (b) is a log–log plot showing $\gamma(\delta, \Omega)$ at the same values of Ω. Again, the asymptotic predictions from equation (S2.15) match extremely well (solid lines).

Furthermore, we find the asymptotic behaviour of $\gamma(\delta, \Omega)$:

$$\gamma(\delta, \Omega) = \frac{1}{4}\Omega A^2 \epsilon + O(\epsilon^2) = \frac{1}{4}\Omega \left[\frac{1}{2}(\Omega - 1) + \frac{\pi}{4}\right]^{-2} \epsilon + O(\epsilon^2), \tag{S2.15}$$

which simplifies in the case $\Omega = 1$ to

$$\gamma(\delta, 1) = 4\pi^{-2}\epsilon + O(\epsilon^2). \tag{S2.16}$$

These predictions match numerical results extremely well, as shown in figure S3.

These values of δ correspond to the lower branch of the relationship between flux and Rayleigh number (see the dashed portion of the curves in figures 5 and 6 in the main paper), so we find that at fixed chimney spacing L, $\mathcal{F}_{\text{Solute}}$ varies with the inverse square of L. In particular, since $\mathcal{F}_{\text{Solute}} = -R_m \gamma(\delta, \Omega)$ and $L = R_m^{-1}\theta_\infty^{-1/2} G(\delta, \Omega)$, we find

$$\mathcal{F}_{\text{Solute}} = -\left[A R_m \theta_\infty\right]^{-1} L^{-2} = -\left[R_m \theta_\infty\right]^{-1} \left[\frac{1}{2}(\Omega - 1) + \frac{\pi}{4}\right] L^{-2}. \tag{S2.17}$$

Perhaps most importantly, this section formalises the argument that the minimum size of the active region required to sustain convection is $\delta = \pi/2$ (independently of Ω). This demonstrates the important physical insight that there must be a finitely wide active region, where baroclinic torque occurs, in order to drive convection through chimneys. It is not the case that the buoyancy causes motion in the chimney and then the rest of the mushy layer responds essentially passively.

S2.3. *Solution for $\delta \gg 1$*

S2.3.1. *Analytical discussion*

Integrating equation (S1.1b), we find

$$\Theta = -\Psi' + c, \tag{S2.18}$$

where $c = \Theta_\delta + \Psi'_\delta = 1 + \Psi'_\delta$. We find numerically that $\Psi'_\delta \to 0$ exponentially: so for now we consider this as an ansatz. If this ansatz holds, then $c \to 1$ exponentially. Note that c is also equal to $\Theta_0 + \Psi'_0$, so with boundary conditions (S1.2a, b)

$$\Theta_0 \sim 1 - \Psi_0^2/\Omega. \tag{S2.19}$$

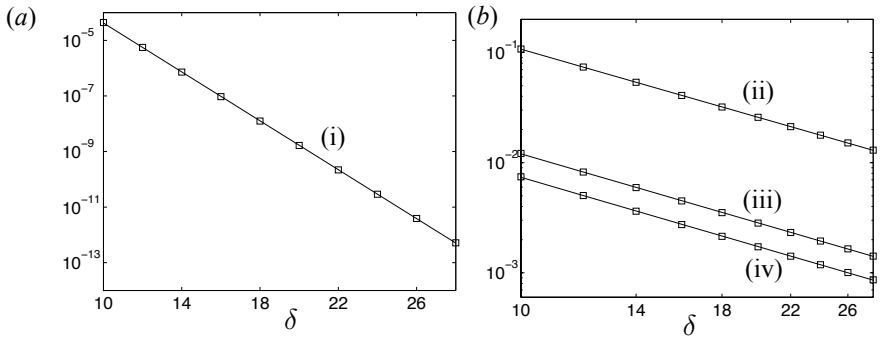

FIGURE S4. (a) is a log–linear plot showing (i) the exponential decay of $-\Psi'_\delta$. The best-fit line is $\Psi'_\delta = -\exp(-1.013\delta + 0.05746)$. ($b$) is a log–log plot showing the algebraic behaviour of (ii) $2 - \Psi_\delta$, (iii) $(\Psi_0)_c - \Psi_0$ and (iv) $\Theta_0 - (\Theta_0)_c$. The best-fit lines are (ii) $\Psi_\delta = 2 - 12.11 \times \delta^{-2.053}$, (iii) $\Theta_0 = (\Theta_0)_c + 1.453 \times \delta^{-2.082}$ and (iv) $\Psi_0 = (\Psi_0)_c - 0.9013 \times \delta^{-2.088}$. Throughout $\Omega = 1$.

If we substitute equation (S2.18) back into (S1.1a), then we find

$$\Psi''' + \Psi\Psi'' + \Psi'(c - \Psi') = 0. \tag{S2.20}$$

Consistently with the exponential decay of Ψ'_δ, this equation can be approximated at large η by

$$\Psi''' + \Psi_\delta\Psi'' + \Psi' = 0, \tag{S2.21}$$

which we can solve by positing the solution $\Psi' = \mathrm{e}^{m\eta}$. This implies

$$m^2 + m\Psi_\delta + 1 = 0 \Rightarrow m = -\frac{\Psi_\delta}{2} \pm \mathrm{i}\sqrt{1 - \left(\frac{\Psi_\delta}{2}\right)^2}. \tag{S2.22}$$

Let $\omega = \sqrt{1 - (\Psi_\delta/2)^2}$. Then

$$\Psi' = \mathrm{e}^{-\eta\Psi'_\delta/2}(A\cos\omega\eta + B\sin\omega\eta). \tag{S2.23}$$

From figure S1, we observe that the first branch has precisely one turning point $\Psi' = 0$. This is consistent with $\omega \to 0$, or equivalently $\Psi \to 2$ from below. Numerically, we observe that this is an algebraic process. Then equation (S2.23) shows that our assumptions are self-consistent and $\Psi'_\delta \sim \mathrm{e}^{-\delta}$.

S2.3.2. *Numerical results*

We numerically integrate the equations to a high accuracy and find that the scalings postulated on the basis of analytical arguments hold very well. We also find that Ψ_δ approaches 2 from below in an inversely quadratic fashion, and find the behaviour of Ψ_0 and Θ_0. These tend to a constant value, which depends on Ω. This value can be found most readily by integrating the equations to large δ subject to $\Psi_\delta = 2$, $\Theta_\delta = 1$. When $\Omega = 1$, we find $[(\Psi_0)_c, (\Theta_0)_c] = [0.8216, 0.3250]$. Figure S4 shows our numerical results.

S2.3.3. *Conclusions*

Numerically we can calculate the various pre-factors, which depend on Ω. However, it is more instructive to fix Ω, so in this subsection, '$\sim$' includes a proportionality constant

that could be determined in terms of Ω. Asymptotically as $\delta \to \infty$

$$G(\delta) \sim \mathrm{e}^{3\delta/2}, \tag{S2.24}$$

$$\gamma(\delta) \sim \mathrm{e}^{-\delta}. \tag{S2.25}$$

High values of δ correspond to the upper branch of the relationship between flux and Rayleigh number (see the solid curves in figures 6 and 7 in the main paper). Now $L = R_m^{-1}\theta_\infty^{-1/2}G(\delta,\Omega)$ so at fixed L, high values of R_m correspond to high values of δ. So $R_m \gg 1$ corresponds to $\delta \gg 1$ and so at high Rayleigh number

$$L \sim R_m^{-1}\theta_\infty^{-1/2}\mathrm{e}^{3\delta/2} \tag{S2.26}$$

implies that

$$\mathcal{F}_{\mathrm{Solute}} \sim -R_m^{1/3}\theta_\infty^{-1/3}L^{-2/3}, \tag{S2.27}$$

since $\mathcal{F}_{\mathrm{Solute}} = -R_m\gamma(\delta,\Omega) \sim -R_m\mathrm{e}^{-\delta}$. So at fixed chimney spacing, flux scales with the cube root of Rayleigh number, and at fixed Rayleigh number, flux scales with chimney spacing to -2/3 power. Therefore, at large chimney spacing, the solute flux decreases with $L^{-2/3}$. To our knowledge, this result has not been observed before, which may be because having one convecting cell in a large region between two chimneys is unstable to the formation of new convecting cells and new chimneys.

S2.4. *Discussion – asymptotics and the maximum-flux criterion*

These asymptotic limits elucidate a number of important features of the Chimney-Active-Passive-Zone model, particularly the need for an active region, and the eventual decrease of solute flux with L. Numerical calculations of G for intermediate values of δ, shown in the main paper and reproduced in figure S5, additionally show that there is a global minimum value of G, which corresponds to the minimum chimney spacing required to sustain convection, and that γ is a bounded, positive function on $\pi/2 < \delta < \infty$. Let δ_m, which depends on Ω, be such that $\partial G/\partial\delta(\delta_m,\Omega) = 0$, and let $G_{\mathrm{min.}}$ be the minimum value of G. Then the minimum chimney spacing is

$$L_{\mathrm{min.}} = R_m^{-1}\theta_\infty^{-1/2}G_{\mathrm{min.}}(\Omega). \tag{S2.28}$$

Combined with our asymptotic observations, this shows that there is some δ_c which maximises the flux on $\delta_m < \delta_c < \infty$. We prove the uniqueness of the maximum in section S3 for the case $\Omega \gg 1$, but numerically we find that this holds in general.

S3. Asymptotic solution in the limit $\Omega \to \infty$

In the limit $\Omega \to \infty$, we can solve the leading-order problem entirely analytically. This allows us to prove that there is a unique chimney spacing that maximises the solute flux, a result which we find numerically for all Ω.

S3.1. *Leading order solution*

At large values of Ω, the solution of the governing equations (S1.1) is a weak departure from the exact solution of no flow, discussed in section S2.2. Considering the boundary conditions (S1.2a, b) at ($\eta = 0$) leads us to posit a regular expansion

$$\Psi = \Psi_0 + \frac{1}{\Omega}f(\eta) + O(\Omega^{-2}), \tag{S3.1}$$

$$\Theta = 1 - \frac{1}{\Omega}g(\eta) + O(\Omega^{-2}). \tag{S3.2}$$

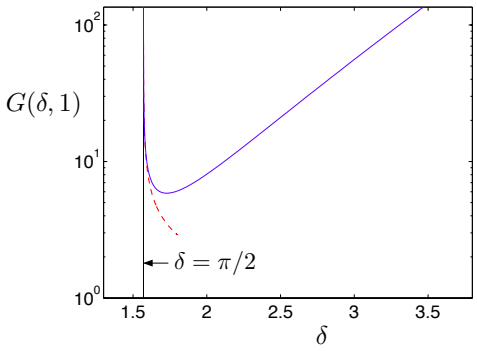

FIGURE S5. Adaptation of figure 7(a) from the main paper, showing $G(\delta, \Omega = 1)$, which is proportional to the chimney spacing. The global minimum corresponds to the minimum chimney spacing required to sustain convection. The asymptotic results derived in this supplementary material for $\delta \to \pi/2$ (dashed red curve) follow the numerical results (solid blue curve) very well. However, the $\delta \gg 1$ results (not shown) only apply for much higher values of δ (see figure S4).

We substitute into the differential equations (S1.1) and find that

$$g'' + \Psi_0 g' + f' = 0, \qquad f'' = g'. \tag{S3.3a, b}$$

The boundary conditions (S1.2) imply that

$$f = 0, \quad f' = \Psi_0^2, \quad g' = -\Psi_0 \quad (\eta = 0), \qquad g = 0, \quad g' = 0 \quad (\eta = \delta), \tag{S3.4$a-e$}$$

Integrating equation (S3.3b), we obtain

$$f' = g - C, \tag{S3.5}$$

where C is a constant, and substituting this into equation (S3.3a), we obtain

$$g'' + \Psi_0 g' + g = C. \tag{S3.6}$$

This has general solution

$$g = \left[A \sin\left(\eta\sqrt{1 - \Psi_0^2/4}\right) + B\cos\left(\eta\sqrt{1 - \Psi_0^2/4}\right)\right] e^{-\Psi_0\eta/2} + C. \tag{S3.7}$$

The boundary condition (S3.4b) with equation (S3.5) shows that

$$B = \Psi_0^2, \tag{S3.8}$$

and then boundary condition (S3.4c) shows that

$$A = \left(\frac{\Psi_0^2}{2} - 1\right) \frac{\Psi_0}{\sqrt{1 - \Psi_0^2/4}}. \tag{S3.9}$$

Boundary condition (S3.4e) then determines the unknown Ψ_0, which is expressed implicitly by

$$\delta(\alpha) = \frac{\arcsin\alpha + \pi(1 + 2n)/2}{(1 - \alpha^2)^{1/2}}, \tag{S3.10}$$

where $\alpha = \Psi_0/2$, n is an integer and arcsin takes its principal value. These multiple solutions, shown in figure S6, correspond to the multiple solutions discussed previously. We restrict attention to $\alpha \geqslant 0$ (such that flow is from the mush into the chimney). Furthermore, there are no solutions if $\alpha \geqslant 1$, so we need consider only $0 \leqslant \alpha < 1$.

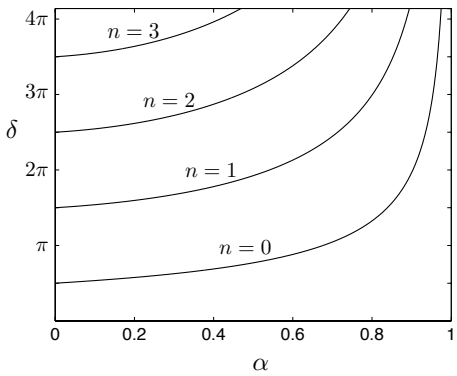

FIGURE S6. Plot of solution curves for equation (S3.10) for the first four branches. Note that there are no solutions for $\delta < \pi/2$ as we found previously.

Finally, C can then be determined from boundary condition (S3.4d). In particular,

$$C = (-1)^n 2\alpha \exp(-\alpha\delta). \tag{S3.11}$$

However, recognising that $\Psi'_\delta = f'(\delta)/\Omega = -C/\Omega$, we can restrict attention to the case n even, thereby ensuring that $\Psi'_\delta < 0$, as discussed previously in section S1.2. Then equation (S1.6) implies that

$$\gamma(\delta, \Omega) = C/2\Omega, \tag{S3.12}$$

so, under the maximum-flux principle, we maximise $C(\delta)$, plotted in figure S7, in order to determine the solute flux, which is proportional to γ.

S3.2. *Application of the maximum-flux criterion and discussion*

As discussed above, we can restrict attention to the domain $0 \leqslant \alpha < 1$, and since $\delta = \delta(\alpha)$ on each branch (as specified by equation S3.10), we can also consider C as a function of α. Now

$$\frac{dC}{d\delta} = \left(\frac{d\delta}{d\alpha}\right)^{-1} \frac{dC}{d\alpha} = \frac{1}{\delta'} \left(1 - \alpha(\alpha\delta)'\right) 2\exp(-\alpha\delta). \tag{S3.13}$$

But

$$\delta'(\alpha) = \frac{1}{1-\alpha^2} + \alpha \frac{\arcsin\alpha + \pi(1+2n)/2}{(1-\alpha^2)^{3/2}} > 0, \tag{S3.14}$$

which, by substituting (S3.14) into (S3.13), shows that $dC/d\delta = 0$ if and only if

$$1 - 2\alpha^2 = \frac{\alpha}{(1-\alpha^2)^{1/2}} (\arcsin\alpha + \pi(1+2n)/2). \tag{S3.15}$$

Now the left-hand side decreases monotonically from 1 to -1 and the right-hand side increases monotonically from 0 to $+\infty$, so by the Intermediate-Value Theorem, there is a unique solution, $\alpha = \alpha_c$, to equation (S3.15). Further, the positive function $C(\alpha)$ satisfies $C(0) = C(1) = 0$, so this turning point must be a maximum. Having solved equation (S3.15) numerically to find α_c, we determine

$$\delta_c = \delta(\alpha_c) = 1/\alpha_c - 2\alpha_c, \tag{S3.16}$$

$$C_c = C(\alpha_c) = 2\alpha_c \exp(-1 + 2\alpha_c^2). \tag{S3.17}$$

Therefore, we have proved the existence of a unique maximum flux on each branch

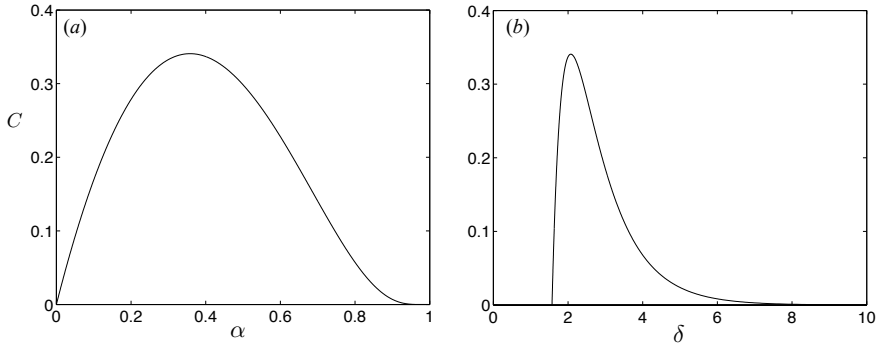

FIGURE S7. The existence of a unique maximum flux, illustrated for the case $n = 0$, which is the overall maximum-flux case. C can be interpreted as a function of α, as in (a), or δ, as in (b).

of solutions. Furthermore, the overall maximum occurs when $n = 0$, which we prove as follows. Define

$$h(\alpha) = (1/\alpha - 2)(1 - \alpha^2)^{1/2} - \arcsin(\alpha), \tag{S3.18}$$

which implies that

$$h'(\alpha) = -(4 + 1/\alpha^2)(1 - \alpha^2)^{1/2} < 0. \tag{S3.19}$$

But $h(\alpha)$, which decreases from $+\infty$ to $-\pi/2$ over $[0, 1)$, satisfies

$$h(\alpha_c) = \pi(1 + 2n)/2, \tag{S3.20}$$

and so as n increases, α_c decreases. Then $C_c = 2\alpha_c \exp(-1+2\alpha_c^2)$ must also decrease with n. Therefore, solutions with a greater number of convecting cells have a lower associated solute flux, and the maximum-flux criterion leads us to consider solutions which have only one convecting cell.

In the case $n = 0$, we find $\alpha_c = 0.3582$, $\delta_c = 2.0749$, and $C_c = 0.3407$. This leads to the asymptotic prediction

$$\gamma_c(\Omega) \sim 0.1704\,\Omega^{-1} \tag{S3.21}$$

for the proportionality constant in the relation $\mathcal{F}_{\text{Solute}} = -R_m\gamma_c(\Omega)$, as is confirmed by the numerical calculations presented in the main paper (see figure 8*a*).

This asymptotic limit proves the uniqueness of a the flux-maximising chimney spacing in the limit $\Omega \gg 1$. However, this result actually holds for all Ω. Indeed, this asymptotic calculation captures a number of features relevant to all values of Ω. In particular, figure S6 is structurally the same as a projection of the dashed curves in figure S2, which is the case $\Omega = 1$. Furthermore, a graph of $\gamma(\delta, \Omega)$ along the first branch of solutions in figure S2 corresponds to figure S7. Thus this asymptotic proof provides valuable corroboration of our numerical observation that there is always a unique value of δ, and hence of L such that the solute flux is maximised, and that we need only consider solutions with one convecting cell.